ELSEVIER

Water Research 38 (2004) 1642–1650

WATER RESEARCH

www.elsevier.com/locate/watres

Light-absorption ratio variation approach to determination of nickel (II) in ng/ml level with 1, 5-di(2-hydroxy-5-sulfophenyl)-3-cyanoformazan

Hong-Wen Gao[a,*], Si-Qing Xia[a], Hong-Yan Wang[b], Jian-Fu Zhao[a]

[a] *School of Environmental Science and Engineering, Tongji University, State Key Laboratory of Pollution Control and Resource Reuse, Shanghai 200092, People's Republic of China*

[b] *Department of Chemistry and Biology, Suzhou Teachers College, Suzhou 234000, People's Republic of China*

Received 28 July 2003; received in revised form 29 October 2003; accepted 22 November 2003

Abstract

The light-absorption ratio variation approach (LARVA) has been described and applied to the quantitative detection of ultramicro amounts of Ni by spectrophotometry, which raises notably the detection sensitivity. The complexation between 1, 5-di(2-hydroxy-5-sulfophenyl)-3-cyanoformazan (DSPCF) and Ni(II) at pH 9.11 was investigated and the binary complex was characterized by the spectral correction technique. Results have shown that ΔA_r^{-1} (ΔA_r—light-absorption ratio variation) is linear in the range of Ni(II) between 5 and 200 ng/ml. The limit of detection (3σ) of Ni(II) is only 1.3 ng/ml. The complexation is selective in the presence of fluoride, hexametaphosphate, ethylene diamine tetraacetate and thioglycollic acid. It has been applied to analysis of water quality with satisfactory results.

Keywords: Light-absorption ratio variation approach; Spectrophotometry; 1, 5-di(2-hydroxy-5-sulfophenyl)-3-cyanoformazan; Characterization of complex; Determination of Ni in ultramicro level

1. Introduction

Spectrophotometry is an ancient but conventional approach in trace analysis. Since last century, it is always applied extensively and studied, particularly in the developing countries. Because a number of limitations appear in aspects of on-line and real-time analysis, automatic, microminiaturization, multi-components detection and not enough sensitivity, many improvement methods are increasingly proposed [1–8], for example development of new instrument, application of chemometrics and computation and instruments' coupling. Besides, lots of highly sensitive chromophores are synthesized and applied [9,10] for the same purpose above. During 1992 and 1998, the progress of "ultraviolet and light absorption spectrometry" was reviewed [11–13]. Recently, a new technique named light-absorption ratio variation approach (LARVA) was established and just applied to determination of Co(II) [14]. It is different from the absorbance ratio method which is often applied to examine the purity of an organic compound or to identify its structure, e.g. drug [15], protein [16]. Both the deep-color chromophore and highly sensitive spectrophotometer supply LARVA with the hardware bases. It makes the analytical sensitivity and accuracy a significant improvement because of a wider linear detection scope and a much lower detection limit. It is quite suitable for analysis of a micro-volume sample, e.g. biologic, wastewater, noble metal and drug. The chromophore, 1, 5-di(2-hydroxy-5-sulfophenyl-)-3-cyanoformazan (DSPCF) is one deep colorant with a high molar absorptivity, $\varepsilon^{540\ nm} = 2.01 \times 10^4$ l/molcm at pH 9.11 so it is fit to the LARVA. From its structure showed in Fig. 1, it is one of cyanoformazans as a typical multitooth ligand and it may bind Cu(II), Fe(II),

*Corresponding author. Tel./fax: +86-21-6598-8598.
E-mail address: hwgao@mail.tongji.edu.cn (H.-W. Gao).

0043-1354/$ - see front matter
doi:10.1016/j.watres.2003.11.030

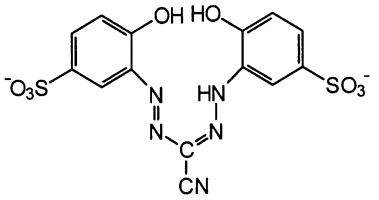

Fig. 1. Structural graph of DSPCF.

Zn(II), Mn(II), Co(II), Al(III) and Pb(II) to form binary complexes. However, we found that the complexation between Ni(II) and DSPCF is sensitive at pH 9.11 and selective in the presence of hexametaphosphate, ethylene diamine tetraacetate (EDTA) and thioglycollic acid. Therefore, the LARVA has been applied to the quantitative detection of Ni(II) in ng/ml level. The applicability is the linear scope from 5 to 200 ng/ml Ni(II) and the detection limit only 1.33 ng/ml. Also, the operation is sample and the instrument is available easily. Therefore, this method is more excellent than the previous conventional techniques, e.g. AAS [17], spectrophotometry [18], electrochemical analysis [19]. In addition, the binary complexation was characterized by the spectral correction technique [11], which has been confirmed to be useful in the elimination of excess of the color reactant and useful in characterization of a chemical reaction, e.g. ligand–metal complexation [20], small molecules–biomacromolecule interaction [21,22].

2. Principle and calculation

2.1. Determination of stepwise stability constant (K_n)

In the earlier determination of the stepwise stability constants ($K_1, \ldots, K_n, \ldots, K_N$) of a ligand (L)–metal (M) complex (ML_N) (N-maximal coordination number), the repetitive measurement of only single solution was designed. Thus, it is possible for K_n to bring an assignable error. Here, the multi-points measurement method was established and the accurate determination of K_n can be made by the linear regression. To see the complexation between L and M illustrated in Fig. 2 and its stepwise reactions:

$$\mathrm{L} + \mathrm{M} \rightleftharpoons^{K_1} \mathrm{ML},$$
$$\mathrm{L} + \mathrm{ML} \rightleftharpoons^{K_2} \mathrm{ML}_2,$$
$$\cdots\cdots$$
$$\mathrm{L} + \mathrm{ML}_{n-1} \rightleftharpoons^{K_n} \mathrm{ML}_n,$$
$$\cdots\cdots$$
$$\mathrm{L} + \mathrm{ML}_{N-1} \rightleftharpoons^{K_n} \mathrm{ML}_N,$$

the effectively complexed fraction (η) of L and the complexation ratio (γ) of L to M are determined and

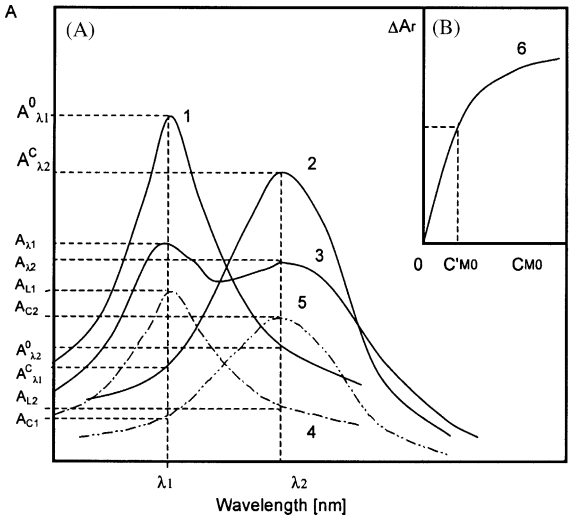

Fig. 2. (A) Sketch of absorption spectra for the establishment of LARVA: (1) L solution, (2) ML complex solution without free L, (3) M–L reaction solution, (4) virtual spectrum of excess of L in 3 and (5) virtual spectrum of ML complex formed in 3 solution. (B) Plots ΔA_r vs. C_{M0}.

calculated by the relations:

$$\eta = \frac{A_{c2} - A_{\lambda 2}}{A^0_{\lambda 2}} + 1 \tag{1}$$

and

$$\gamma = \eta \times \frac{C_{L0}}{C_{M0}}, \tag{2}$$

where

$$A_{c2} = \frac{A_{\lambda 2} - \beta A_{\lambda 1}}{1 - \alpha\beta}, \tag{3}$$

where the symbols C_{M0} are C_{L0} are the initial concentrations of M and L. From Fig. 3, A_{c2} indicates the real absorbance of only the M–L complex at wavelength λ_2 against water, which cannot be measured directly. $A^0_{\lambda 2}$ is the absorbance of the L solution measured at λ_2 against water. The symbols $A_{\lambda 2}$ and $A_{\lambda 1}$ are the absorbances of the M–L solution, respectively, measured at λ_2 and λ_1 against water. Both β and α are the correction constants and they may be calculated from curve 1 and 2 by means of

$$\beta = \frac{A^0_{\lambda 2}}{A^0_{\lambda 1}} \tag{4}$$

and

$$\alpha = \frac{A^C_{\lambda 2}}{A^C_{\lambda 1}}. \tag{5}$$

The M–L solution with γ of L to M between $n-1$ and n mostly consists of both ML_{n-1} and ML_n complexes and the free L, especially in $n - 0.7 < \gamma < n - 0.3$. Thus, the other complexes ML_{n-2} and ML_{n+1} only occupy too little fraction to affect the determination of K_n. The n-

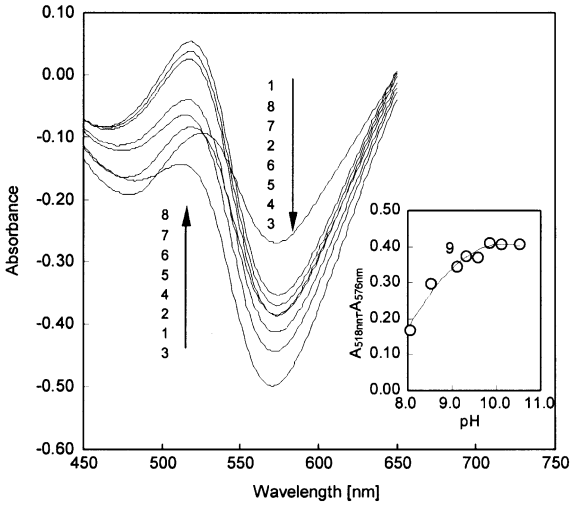

Fig. 3. Effect of pH on the absorption spectra of the Ni-DSPCF solutions, all of which contained 0.40 μmol of DSPCF, 10.00 μg of Ni(II) and 20 mg of EDTA and measured against the reagent blank without Ni(II): From spectrum (1) to (8) pH 8.05, 8.52, 9.11, 9.33, 9.59, 9.85, 10.11 and 10.52. (9) Variation of the absorbance difference of the above solutions between peak and valley with pH. All the solutions were 11.0 ml.

step stability constant (K_n) of complex ML_N is calculated by the relation:

$$y = K_n x, \tag{6}$$

where

$$x = C_{L0} - \gamma C_{M0}$$

and

$$y = \left(\frac{1}{n-\gamma} - 1\right)$$

(recommending : $n - 0.7 < \gamma < n - 0.3$).

Therefore, each K_n can be determined by varying the molarity of L in M (constant molarity) solution. From all K_n the cumulative stability constant (K) of ML_N is calculated by

$$K = \prod_{n=1}^{N} K_n. \tag{7}$$

2.2. Light-absorption ratio variation approach

The complex reactions above between L and M is merged as follows:

	$n\mathbf{L}$	+	$\mathbf{M}$	$\rightleftharpoons$	$\mathbf{ML}_n$.
Initiation	C_{L0} ($A^0_{\lambda_1}$ at λ_1 and $A^0_{\lambda_2}$ at λ_2)		C_{M0}		0.
Equilibrium	$C_L = C_{L0} - nC_{M0}$ (A_{L1} at λ_1 and A_{L2} at λ_2)		$C_M \to 0$		C_{M0} (A_{C1} at λ_1 and A_{C2} at λ_2).

From the illustrations shown in Fig. 2(A).

$$A_{\lambda 1} = A_{L1} + A_{C1}$$

and

$$A_{\lambda 2} = A_{L2} + A_{C2},$$

$$A_r = \frac{A_{\lambda 2}}{A_{\lambda 1}} = \frac{A_{L2} + A_{C2}}{A_{L1} + A_{C1}} = \frac{\delta C_L \varepsilon^L_{\lambda 2} + \delta C_{M_0} \varepsilon^{ML}_{\lambda 2}}{\delta C_L \varepsilon^L_{\lambda 1} + \delta C_{M_0} \varepsilon^{ML}_{\lambda 1}},$$

$$A_{r0} = \frac{A^0_{\lambda 2}}{A^0_{\lambda 1}} = \frac{\delta C_{L0} \varepsilon^L_{\lambda 2}}{\delta C_{L0} \varepsilon^L_{\lambda 1}},$$

$$A_r - A_{r0} = \frac{C_L \varepsilon^L_{\lambda 2} + C_{M_0} \varepsilon^{ML}_{\lambda 2}}{C_L \varepsilon^L_{\lambda 1} + C_{M_0} \varepsilon^{ML}_{\lambda 1}} - \frac{\varepsilon^L_{\lambda 2}}{\varepsilon^L_{\lambda 1}},$$

$$\Delta A_r = \frac{(\varepsilon^L_{\lambda 1} \varepsilon^{ML}_{\lambda 2} - \varepsilon^L_{\lambda 2} \varepsilon^{ML}_{\lambda 1}) C_{M0}}{(C_{L0} - nC_{M0})(\varepsilon^L_{\lambda 1})^2 + C_{M0} \varepsilon^{ML}_{\lambda 1} \varepsilon^L_{\lambda 1}},$$

$$\Delta A_r^{-1} = \frac{C_{L0}(\varepsilon^L_{\lambda 1})^2}{\varepsilon^{ML}_{\lambda 2} \varepsilon^L_{\lambda 1} - \varepsilon^{ML}_{\lambda 1} \varepsilon^L_{\lambda 2}}, C^{-1}_{M0} + \frac{\varepsilon^L_{\lambda 1}(\varepsilon^{ML}_{\lambda 1} - n\varepsilon^L_{\lambda 1})}{\varepsilon^{ML}_{\lambda 2} \varepsilon^L_{\lambda 1} - \varepsilon^{ML}_{\lambda 1} \varepsilon^L_{\lambda 2}},$$

$$\therefore \Delta A_r^{-1} = p' C^{-1}_{M0} + q', \tag{8}$$

where

$$p' = \frac{C_{L0}(\varepsilon^L_{\lambda 1})^2}{\varepsilon^{ML}_{\lambda 2} \varepsilon^L_{\lambda 1} - \varepsilon^{ML}_{\lambda 1} \varepsilon^L_{\lambda 2}} \quad \text{and}$$

$$q' = \frac{\varepsilon^L_{\lambda 1}(\varepsilon^{ML}_{\lambda 1} - n\varepsilon^L_{\lambda 1})}{\varepsilon^{ML}_{\lambda 2} \varepsilon^L_{\lambda 1} - \varepsilon^{ML}_{\lambda 1} \varepsilon^L_{\lambda 2}}.$$

Both p' and q' are constants.

The symbols $\varepsilon^L_{\lambda 1}$, $\varepsilon^L_{\lambda 2}$, $\varepsilon^{ML}_{\lambda 1}$ and $\varepsilon^{ML}_{\lambda 2}$ are the molar absorptivities of L and ML at λ_1 and λ_2 and δ is the cell thickness (cm). The sketch curve of Eq. (8) is shown in Fig. 2(B). Plot ΔA_r vs. C_{M0} is linear when the molarity of M is much less than that of L, e.g. C'_{M0}. Thus, Eq. (8) is rewritten as

$$\Delta A_r = pC_{M0} + q, \tag{9}$$

where the symbols p and q are constants. Eqs. (8) and (9) both can be directly used in quantitative detection of M traces. This method is named as light-absorption ratio variation approach (LARVA). From the equation above, the sensitivity factor p^{-1} is the inverse ratio to C_{L0}. Therefore, less L is added and higher the analytical sensitivity goes. Nevertheless, too low L will certainly bring an obvious error, e.g. increase of fraction of the instrument's noise signal. Therefore, the higher the light absorptivity of a chromophore is and the more sensitive the spectrometer is, the lower the detection limit of a component goes by LARVA. According to the present cases, it is suggested for the addition of a chromophore to produce the peak absorbance between 0.05 and 0.2.

3. Experimental section

3.1. Apparatus and reagents

Absorption spectra were recorded on a TU1901 spectrophotometer (PGeneral, Beijing). The pH of the solution was measured with a Model delta 320 pH-meter (Mettler Toledo Group, Shanghai). A Model BS110S electronic balance (Sartorius Instruments, Beijing) was used to accurately weight the standard substances and DSPCF. A Model TAS-986 flame atomic absorption spectrometer (PGeneral, Beijing) was used to examine the accuracy of the LARVA by analyzing water samples.

Stock standard solution of Ni(II) (100 mgl/l) was prepared by dissolving metal nickel in spectrometric purity in 20% hydrogen chloride and diluting with deionized water. Both 0.100 and 1.00 mg/l Ni(II) standard solutions were prepared daily by diluting the above solution. Standard DSPCF (0.800 mmol/l) solution was prepared by dissolving 243 mg of disodium 1, 5-di(2-hydroxy-5-sulfophenyl)-3-cyanoformazan (content 80%, provided by Changke Reagents Institute of Shanghai) in 500 ml deionized water. It was used to complex Ni(II). DSPCF use solution, 0.200 mmol/l was prepared daily and it was used in determination of Ni(II). The ammonium buffer solutions at pH 8.05, 8.52, 9.11, 9.33, 9.59, 9.85, 10.11 and 10.52 were prepared with ammonia water and ammonium chloride. The first masking reagent was prepared by mixing 3% hexametaphosphate, 3% ammonium fluoride and 3% ascorbic acid to mask Co(II), Al(III), Mn(II), Fe(II) and Fe(III) from interfering the complexation. This solution must be added before the color reaction.

The second masking reagent was prepared by mixing 2% Na_2EDTA and 2% thioglycollic acid and it was used to mask Zn(II), Cu(II), Pb(II), Cr(III), Cd(II), Hg(II) and Al(III). This solution must be added after accomplishment of the complexation. Otherwise, it will complex Ni(II) competitively.

3.2. General procedures

Characterization of Ni-DSPCF complex. Into a group of 10-ml calibrated flasks, 1 ml of pH 11 buffer solution and 2.00 μg of Ni(II) and 0.800 mmol/l DSPCF from 0.020 to 0.120 μmol were added and then diluted to 10.0 ml. After 10 min, 1 ml of the second masking reagent was added. After mixing for 5 min, the absorbances were measured at 576 and 518 nm against the blanks without Ni(II). The factors, A_c, η, γ, $\varepsilon_n^{518\ nm}$, K_n and K all were calculated by the equations above and by the linear regression.

Determination of ultramicro amounts of Ni(II). 5.00 ml of a water sample was added into 10-ml flask. 1 ml of the first masking reagent, 1 ml of pH 9.11 buffer solution and 0.500 ml of 0.200 mmol/l DSPCF were added. Diluted to 10.0 ml and mixed well. After 10 min, 1.00 ml of the second masking reagent were added. After 5 min, the absorbances ($A_{518\ nm}$ and $A_{576\ nm}$) were measured at 518 (λ_2) and 576 nm (λ_1) against water. Simultaneously, a reagent blank without Ni(II) was prepared and then to measured $A^0_{518\ nm}$ and $A^0_{576\ nm}$. Thus, ΔA_r is calculated by the relation:

$$\Delta A_r = \frac{A_{518\ nm}}{A_{576\ nm}} - \frac{A^0_{518\ nm}}{A^0_{576\ nm}}. \quad (10)$$

From Eq. (8) or (9), C_{Ni} in a sample was calculated.

4. Results and discussion

4.1. Effect of pH on absorption spectra

The absorption spectra of the Ni-DSPCF solutions in various pH mediums were shown in Fig. 3. From 8 spectra and curve 9, by comparing the absorbance's difference between peak and valley, the complexation between DSPCF and Ni(II) is sensitive when pH is more than 9.0. If the solution is too basic, the precipitation of hydroxide will occur. On the contrary, the complexation goes insensitive. In this work, pH 9.11 was specified and used. From curve 3, the absorption peak is located at 518 nm and the valley at 576 nm. Such two wavelengths were used in quantitative detection of Ni(II) so as to obtain a maximal ΔA_r.

4.2. Characterization of Ni-DSPCF complex

Variation of the light-absorption ratio, $A_{576\ nm}/A_{518\ nm}$ of the Ni-DSPCF solutions at pH 9.11 is shown as curve 1 in Fig. 4. The ratios approach a minimum and remains constant when the addition of Ni(II) is more than 0.85 time of DSPCF. It states that the DSPCF is almost complete to complex Ni(II) and only a color compound, Ni-DSPCF complex exists in the solution in the presence of enough excessive Ni(II). The absorption spectrum of such a solution is shown as curve 2 in Fig. 4. From curve 2, the absorption peak of the Ni-DSPCF complex is located at 522 nm. From curve 3, we observe that the background compound, DSPCF has a strong light-absorption between 450 and 600 nm. Therefore, it is fit to LARVA. Its absorption peak is located at 540 nm. The spectral peak of the Ni-DSPCF complex appears for 18 nm of blue shift. The break point approach [23] was used to estimate the composition ratio of Ni(II) to DSPCF to be 0.5 : 1. The complex $Ni(DSPCF)_2$ was formed possibly, which will be confirmed below. From curves 2 and 3, the correction coefficients were calculated to be $\beta_{518\ nm/576\ nm} = 1.078$ and $\alpha_{576\ nm/518\ nm} = 0.270$ and they will be used to calculate η, γ and C_L below.

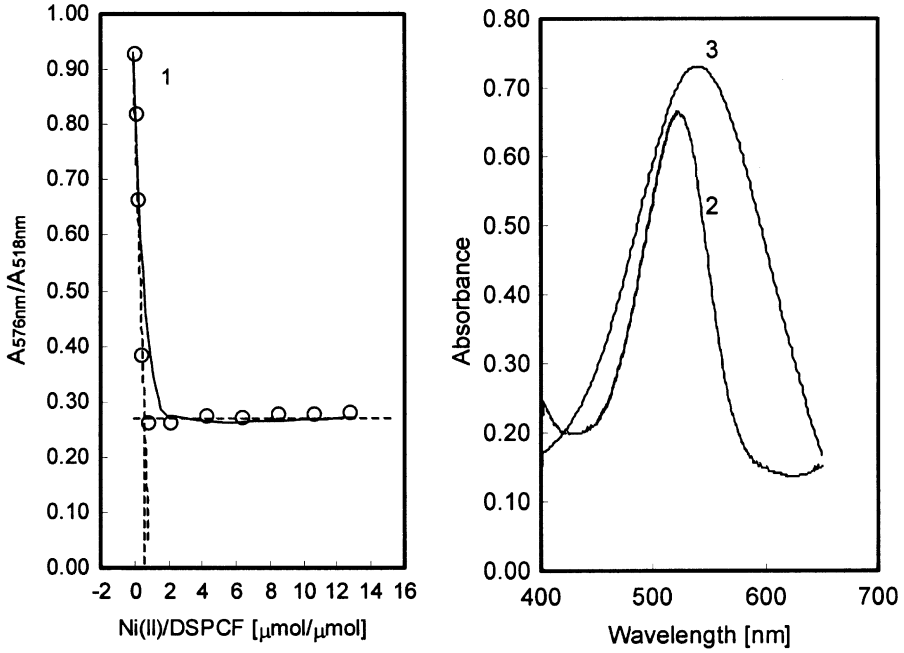

Fig. 4. Formation of the Ni-DSPCF complex where both the solutions no longer contained the excess of DSPCF at pH 9.11 in the presence of 20 mg of EDTA: (1) variation of $A_{576\ \mathrm{nm}}/A_{518\ \mathrm{nm}}$ with the initial molar ratio of Ni(II) to DSPCF initially containing 0.40 μmol, (2) and (3) are the absorption spectra of DSPCF and Ni(DSPCF) complex, respectively both at 0.40 μmol measured against water. All the solutions were 11.0 ml.

The spectral correction technique has been applied to an accurate and visualized characterization of the Ni-DSPCF complex and its results are shown in Fig. 5. From curve 1, the equilibrium concentration of DSPCF approaches zero if the initial DSPCF is less than 0.005 mmol/l. This is attributed to the fact that DSPCF is much less than Ni(II) molarity. From curve 2, γ of DSPCF to Ni(II) increases with increase of DSPCF molarity and then approaches a maximal constant at 2.0 when DSPCF is more than 0.0075 mmol/l. Therefore, the formation of $Ni(DSPCF)_2$ was confirmed. In addition, the continuous variations [24] method was used to examine the composition ratio of the complex obtained above and it too gave the same result.

From curve 1, η of DSPCF is less than 84% when DSPCF is more than 0.0075 mmol/l. This indicates that over 16% DSPCF is free in the complexation solution. Certainly, it interferes in the measurement of light absorption of the complex. Therefore, an ordinary spectrophotometric method is not suitable for the reaction with a deeply color chromophore. From A_c and γ of each solution, ε of the complex solutions at 518 nm was calculated and the result is shown as curve 3 in Fig. 5. Plots ε vs. γ is linear, so the step-wise molar light absorptivity (ε_n) of the Ni-DSPCF complex was calculated as follows: $\varepsilon_1 = 1.61 \times 10^4$ and $\varepsilon_2 = 3.22 \times 10^4$ l/mol/cm at 518 nm.

By further data-handling and calculation of the characteristic factors of the solutions above and by means of Eqs. (6) and (7), plots y vs. x are shown in Fig. 6 and both of them are linear. From the slopes, the step-wise stability constants of complex $Ni(DSPCF)_2$ were calculated to be $K_1 = 1.75 \times 10^7$ and $K_2 = 7.08 \times 10^6$ l/mol. Therefore, the cumulative $K = 1.24 \times 10^{14}$. Hence, this complex is strongly stable because of the enough high K. The spectral correction technique is simpler in operation and more understandable and more visualized in principle than the classical method e.g. continuous variations [23].

4.3. Application of LARVA

4.3.1. Effect of addition of DSPCF on ΔA_r

From the variation (as shown in Fig. 7) of ΔA_r of the solutions with the constant initial molar ratio of Ni(II) to DSPCF at 0.213 μmol/μmol in the presence of EDTA, ΔA_r approaches a maximal constant only when DSPCF is more than 0.040 μmol. ΔA_r decreases when DSPCF is less than 0.040 μmol. The primary reasons are that the self-aggregation of DSPCF will not occur in an extremely diluted solution and the fraction of the instrumental noise raise. Of course, use of a high-sensitive and low-noise spectrometer will reduce notably the measurement error of the light-absorption ratio.

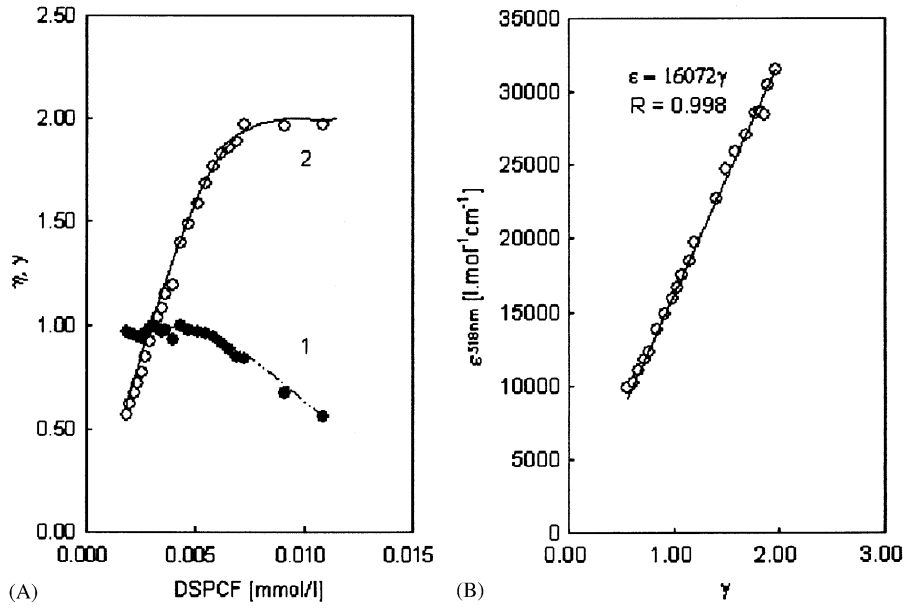

Fig. 5. Variation of η, γ and ε: (1) η of DSPCF, (2) γ of the binding DSPCF to Ni(II) and (3) ε of the Ni-DSPCF complex at 518 nm. All the solutions contained 2.00 μg of Ni(II), 20 mg of EDTA and DSPCF from 0.020 to 0.120 μmol at pH 9.11. All the solutions were 11.0 ml.

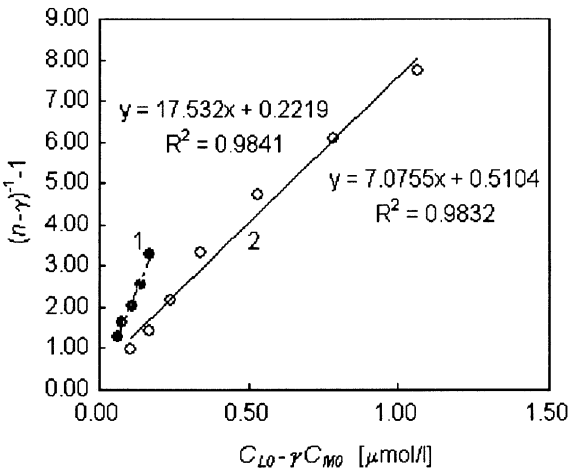

Fig. 6. Determination of the stepwise stability constants (K_n) at pH 9.11 at 20°C: (1) $(1-\gamma)^{-1}-1$ vs. $(C_{L0}-\gamma C_{Ni})$ for K_1 and (2) $1-(2-\gamma)^{-1}-1$ vs. $(C_{L0}-\gamma C_{Ni})$ for K_2 of $Ni(DSPCF)_2$ complex where the solutions are same as those in Fig. 5.

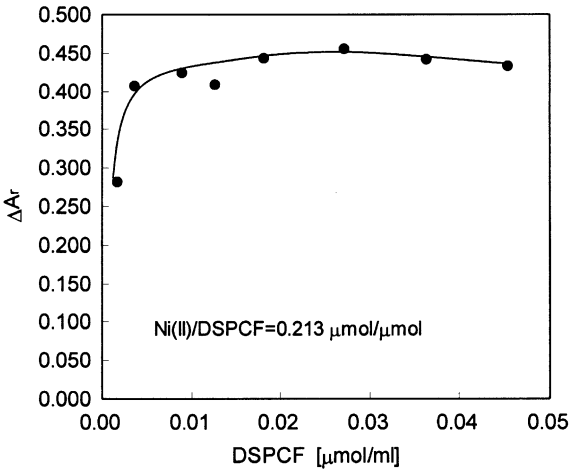

Fig. 7. Effect of DSPCF molarity on ΔA_r of the solutions initially containing DSPCF from 0.020 to 0.500 μmol and Ni(II) from 0.250 to 6.25 μg, where the initial molar ratios of Ni(II) to DSPCF always remain a constant at 0.213 μmol/μmol in the presence of 20 mg of EDTA. All the solutions were 11.0 ml.

4.3.2. Calibration graphs and detection limit of Ni(II)

Four series of standard Ni(II) between 0 and 0.050, 0 and 0.100, 0 and 0.200 and 0 and 0.400 μg/ml were prepared and 1.00, 2.00, 3.00 and 5.00 ml of 0.0400 mmol/l DSPCF were added, respectively. The absorbance of each solution was measured and ΔA_r was calculated by Eq. (10). Their regression equations are given in Table 1. The limit of detection of Ni(II), defined as the blank values plus 3 times the standard deviation of 10 replicated blanks, was calculated and given in Table 1, too. By comparing them, Line 3 owns the lowest limit. Therefore, it is selected in analysis of water quality.

Table 1
Regression equations and detection limit of Ni(II)

Line	Ni(II) (μg/ml)	DSPCF (mM)	p'	q'	ΔA_r^{-1} vs. $C_{Ni(II)}^{-1}$	R[a]	σ[b]	DT[c] (ng/ml)
1	0–0.020	0.002	0.1485	−4.81	$\Delta A_r^{-1} = 0.1485 C_{Ni(II)}^{-1} - 4.81$	0.9983	0.006442	2.8
2	0–0.100	0.004	0.1305	−0.748	$\Delta A_r^{-1} = 0.1305 C_{Ni(II)}^{-1} - 0.748$	0.9998	0.006615	2.5
3	0–0.200	0.010	0.3733	−1.26	$\Delta A_r^{-1} = 0.3733 C_{Ni(II)}^{-1} - 1.260$	0.9994	0.001147	1.3
4	0–0.400	0.020	0.7687	−0.875	$\Delta A_r^{-1} = 0.7687 C_{Ni(II)}^{-1} - 0.875$	0.9998	0.00067	1.5

[a] Linear correlation coefficient.
[b] Standard deviation of 10 repetitive reagent blanks.
[c] Detection limit of Ni(II) was calculated by $DT = 3 \times \sigma \times p'$.

Table 2
Effect of foreign ions on ΔA_r of the solution initially containing 1.00 μg of Ni(II)

No.	Ion added	Added (μg/10 ml)	ΔA_r	Error[a] (%)
1	Ni(II)	1.0	0.3533	0
2	No.1 + Ca(II)	100	0.3674	4.0
3	No.1 + Mg(II)	40	0.3674	4.0
4	No.1 + Al(III)	10	0.3296	−6.7
5	No.1 + Fe(II)	10	0.3950	12
6	No.1 + Fe(III)	10	0.3674	4.0
7	No.1 + Zn(II)	5	0.3439	−2.7
8	No.1 + Mn(II)	20	0.3932	11.3
9	No.1 + Mo(IV)	50	0.3524	−0.3
10	No.1 + Pb(II)	50	0.3702	4.8
11	No.1 + Co(II)	1.0	0.3480	−1.5
12	No.1 + Cd(II)	10	0.3609	2.2
13	No.1 + Ge(IV)	50	0.3559	0.7
14	No.1 + Sn(II)	10	0.3823	8.2
15	No.1 + Cr(III)	20	0.3713	5.1
16	No.1 + Ba(II)	50	0.3627	2.7
17	No.1 + V(V)	10	0.3438	−2.7
18	No.1 + Hg(II)	10	0.3592	1.7
19	No.1 + SDS	100	0.3627	2.7
20	No.1 + acetic acid	100	0.3286	−7.0
21	No.1 + formal	10	0.3681	4.2
22	No.1 + ethanol	100	0.3459	−2.1
23	No.1 + lysine	100	0.3671	3.9
24	No.1 + cystine	100	0.3632	2.8
25	No.1 + glucose	50	0.3752	6.2
26	No.1 + citric acid	20	0.3317	−6.1
27	No.1 + protein	10	0.3236	−8.4

[a] Error $= (\Delta A_r^{No.x} \Delta A_r^{No.1})/\Delta A_r^1 \times 100$ (x is from 2 to 27).

Table 3
Determination of Ni(II) in water samples

Sample no.	Sampled from	Ni(II) found in sample (mg/l)	RSD (%)	Ni(II)[a] (mg/l)
1	Polluted lake water	0.2604	1.81	0.232
		0.2576		
		0.2593		
		0.2628		
		0.2572		
		0.2506		
		0.2580 (±0.0047)[b]		
2	Sewage	0.0382	6.63	0.0419
		0.0431		
		0.0425		
		0.0462		
		0.0457		
		0.0437		
		0.0433 (±0.0029)[b]		
3	Huaihe River	0.0427	2.57	0.0408
		0.0434		
		0.0415		
		0.0437		
		0.0409		
		0.0420		
		0.0424 (±0.0011)[b]		

[a] Average of two replicated determinations by FAAS.
[b] Average of five replicated determinations.

Effect of foreign ions: Five chemical reagents were added in order to mask the other metal ions in the reaction and the recommended procedure in "Experimental Section" was carried out. Twenty-six of foreign ions and substances including 9 organic compounds were added in the Ni(II) complexation solution and their effects on ΔA_r were shown in Table 2. Both Mn(II) and Fe(II) appear in high error over 10% only when their mass concentrations are more than 10 times of Ni(II). Therefore, the recommended method is selective and fit to natural water.

4.3.3. Analysis of water samples

As a test of the method, Ni(II) in three water samples was determined. The results are listed in Table 3. The

recovery rates of Ni(II) added are between 91.0% and 116% and the RSD less than 3.36%. The analytical results were also compared with the results obtained by flame atomic absorption spectrometry (FAAS) [25]. The two methods are uniform so this method is accurate.

5. Conclusions

The LARVA is a great advancement and contribution to spectrophotometric method in ultra-trace analysis. Also, it will improve notably a lot of the present spectrophotometric methods so that they will become more useful in material and environmental analysis, detection of water quality, quality control of industrial products and so on. In characterization of a chemical reaction, the traditional methods are complicated and limited, especially for a reaction with a deep-color reactant. The spectral correction technique may bring the formation constants of a complex a visualized graph and satisfactory result. We believe that it will still play an important role in coordination chemistry, oxidation-reduction reaction, macromolecular assembly and the other relations.

Acknowledgements

Financial support from both the National High Technology Research and Development Program of China (863 Program, No. 2002 AA 601320) and the National Natural Science Foundation of China (No. 50008011) is gratefully acknowledged.

References

[1] Bosch-Reig F, Campins-Falco P, Sevillano-Cabeza A, Herraez-Hernandez R, Molins-Legua C. Development of the H-point standard-additions method for ultraviolet-visible spectroscopic kinetic analysis of two-component systems. Anal Chem 1991;63(21):2424–9.

[2] Gao HW, Li YC, Zhang PF, Tao M, Wang L. Determination of trace amounts of cadmium with *p*-acetyl-benzenediazoaminoazobenzene by primary–secondary wavelength spectrophotometry. J Anal Chem 2001; 56(11):1007–10.

[3] Zolgharnein J, Abdollahi H, Jaefarifar D, Azimi GH. Simultaneous determination of Fe(II) and Fe(III) by kinetic spectrophotometric H-point standard addition method. Talanta 2002;57(6):1067–73.

[4] Mutaftchiev K, Tzachev K. Determination of manganese (II) in some medicinal plants and their decoctions by a kinetic spectrophotometric method. Phytochem Anal 2003;14(3):160–3.

[5] Umemura T, Kasuya Y, Odake T, Tsunoda K. Sensitive measurement of methylene blue active substances by attenuated total reflection spectrometry with a trimethylsilane-modified glass slab optical waveguide. Analyst 2002;127(1):149–52.

[6] Gao HW. Beta-correction spectrophotometric determination of arsenic in waste water with ethyl violet. Talanta 1995;42(5):891–5.

[7] Fábio RP, Rocha P, Martelli B, Boaventura FR. A multicommutation-based flow system for multi-element analysis in pharmaceutical preparations. Talanta 2001; 55(4):861–9.

[8] Amin AS, Issa YM. Ion-association method for the colorimetric determination of neomycin sulphate in pure and dosage forms. Spectrochim Acta Part A: Mol Biomol Spectrosc 2003;59(4):663–70.

[9] Ma H, Wohlers J, Meierhenrich U, Bernecker A, Suling V, Thiemann W. Analysis of oxidative degradation products of 2, 4, 6-trichlorophenol treated with air ions. Anal Chem 2001;73(14):3506–10.

[10] Ma Q, Ma H, Wang Z, Su M, Xiao H, Liang S. A highly selective calyx[4]arene-based chromoionophore for Ni^{2+}. Chem Lett 2001;30(2):100–1.

[11] Hargis LG, Howell JA. Ultraviolet and light absorption spectrometry. Anal Chem 1992;64:66–79.

[12] Hargis LG, Howell JA, Sutton RE. Ultraviolet and light absorption spectrometry. Anal Chem 1996;68(12): 169–84.

[13] Howell JA, Sutton RE. Ultraviolet and light absorption spectrometry. Anal Chem 1998;70(12):107–18.

[14] Gao HW, Wang HY, Zhang SY, Zhao JF. Establishment of light-absorption ratio variation approach and application to determination of Co(II) and novel characterization of Co(II) and Zn(II) complexes with 1, 5-di(2-hydroxy-5-sulfophenyl)-3-cyanoformazan. New J Chem, 2003; 27(11): 1649–56.

[15] Liu SD, Yang Z. Progress of application of pH indicator absorbance ratio method in drug analysis. Chin J Pharm 1995;26(5):231–4.

[16] Murphy JB, Kies MW. Note on spectrophotometric determination of proteins in dilute solutions. Biochem Biophys Acta 1960;45(2):382–4.

[17] Ali A, Ye Y, Xu G, Yin X, Zhang T. Determination of nickel after online sorbent preconcentration by FI-FAAS using dimethylglyoxime as a complexing agent. Microchem J 1999;63(3):365–73.

[18] Vicenta S, Maniasso N, Queiron ZF, Zagatto EAG. Spectrophotometric flow-injection determination of nickel in biological materials. Talanta 2002;57(3):475–80.

[19] Sancho D, Deban L, Campos I, Pardo R, Vega M. Determination of nickel and cobalt in refined beet sugar by adsorptive xathodic stripping voltammetry without sample pretreatment. Food Chem 2000;71(1):139–45.

[20] Gao HW, Chen YS, Li YC. Solution properties of aluminum and titanium complexes with *o*-chlorophenyl-fluorone and competition coordination for selective determination of trace amounts of titanium. Mikrochim Acta 2001;137(3–4):141–8.

[21] Gao HW, Xu WQ. Langmuir aggregation of evans blue on cetyl trimethylammonium bromide and on proteins and application. Anal Chim Acta 2002;458(2):417–24.

[22] Gao HW, Zhao JF. Langmuir aggregation of safranin t in nucleic acids and its application. Aust J Chem 2002; 55(12):767–72.

[23] Gao HW, Hu ZJ, Zhao JF. Investigation of biomacromolecular assembly: substitution reaction occurring in protein. Chem Phys Lett 2003;376(1–2):251–8.

[24] Likussar W. Computer approach to the continuous variations method for spectrophotometric determination of extraction and formation constants. Anal Chem 1973;45(11):1926–31.

[25] ISO. Water quality—determination of cobalt, nickel, copper, zinc, cadmium and lead—flame atomic absorption spectrometric methods, ISO 8288-1986.